Rend. Fis. Acc. Lincei
DOI 10.1007/s12210-013-0248-y

CHIRALITY IN CHEMISTRY AND BIOPHYSICS

Aligned molecules: chirality discrimination in photodissociation and in molecular dynamics

Federico Palazzetti · Po-Yu Tsai · Andrea Lombardi · Masaaki Nakamura · Dock-Chil Che · Toshio Kasai · King-Chuen Lin · Vincenzo Aquilanti

Received: 28 May 2013 / Accepted: 5 July 2013
© Accademia Nazionale dei Lincei 2013

Abstract Emergence of biochemical homochirality is an intriguing topic, and none of the proposed scenarios has encountered a unanimous consensus. Candidates for naturally occurring processes, which may originate chiral selection, involve interaction of matter with light and molecular collisions. We performed and report here: (1) simulations of photodissociation of an oriented chiral molecule by linearly polarized (achiral) light observing that the angular distribution of the photofragments is characteristic of each enantiomer and both differ from the racemic mixture; and (2) molecular dynamics simulations (elastic collisions of oriented hydrogen peroxide, one of the most simple chiral molecules, with Ne atom) demonstrating that the scattering and the recoil angles are specific of the enantiomeric form. The efficacy of non-chiral light (in the case of photodissociation) and of non-chiral projectile (in the case of collisions) is due to the molecular orientation, as an essential requirement to observe chiral effects. The results of the simulations, that we report in this article, provide the background for the perspective realization of experiments which go beyond the well-documented ones involving interaction of circularly polarized laser (chiral light) with the matter, specifically by making use of non-chiral, i.e. linearly polarized or unpolarized light sources, and also by obtaining chiral effects with no use at all of light, but simply inducing them by molecular collisions. The case of vortices is discussed in a companion paper.

Keywords Trajectory simulations · Molecular orientation · Molecular collisions · Enantioselection

This contribution is the written, peer-reviewed, version of a paper presented at the conference "Molecules at Mirror—Chirality in Chemistry and Biophysics", held at Accademia Nazionale dei Lincei in Rome in 29–30 October 2012.

F. Palazzetti (✉) · A. Lombardi · V. Aquilanti
Dipartimento di Chimica, Università di Perugia, via Elce di Sotto, 8, 06123 Perugia, Italy
e-mail: fede_75it@yahoo.it; fede75it@gmail.com

F. Palazzetti
Consiglio Nazionale delle Ricerche, Istituto di Metodologie Inorganiche e dei Plasmi, Bari, Italy

P.-Y. Tsai · M. Nakamura · T. Kasai · K.-C. Lin
Department of Chemistry, National Taiwan University, Taipei, Taiwan

P.-Y. Tsai · M. Nakamura · T. Kasai · K.-C. Lin
Institute of Molecular and Atomic Sciences, Taipei, Taiwan

D.-C. Che
Graduate School of Science, Department of Chemistry, Osaka University, Osaka, Japan

V. Aquilanti
Consiglio Nazionale delle Ricerche, Istituto di Metodologie Inorganiche e dei Plasmi, Rome, Italy

1 Introduction: aligning and orienting molecules

This paper is part of a series of accounts on the manifestation of chiral effects in collisions of aligned molecules. The first paper (Aquilanti et al. 2011a), published in the special issue for the symposium "Astrochemistry: molecules in space and in time" held in Rome at "Accademia dei Lincei" on 4 and 5 November 2010, concerned the collision alignment occurring in supersonic expansions of seeded molecular beams, denominated "natural alignment". The second part, published in this special issue, (Su et al. 2013) focused on the chiral discrimination obtained in vortices produced in gaseous streams. In this report, we

Published online: 25 July 2013

discuss effects arising because of the chirality in photodissociation and molecular dynamics.

Recent discoveries of numerous organic molecules in meteorites, and (surprisingly) in interstellar space, gave rise to the formulation of many hypotheses about the origin of biological selectivity of chirality: we mention random fluctuations, enantioselective synthesis and parity violation (see for example Barron 1986; Quack 2002; Rikken and Raupach 2000; Avalos et al. 1998 and several articles in the proceedings of the previous Symposium "Astrochemistry: molecules in space and in time": Aquilanti et al. 2011b; Bacchus-Montabonel 2011; Gallori 2011, see also Aquilanti et al. 2006, 2008; as well as in this issue: Barron 2013; Longo and Coppola 2013; Ribó et al. 2013). Of particular interest is the observation that chiral discrimination can be induced by whirling motions in liquids and in the formation of aggregates of achiral porphyrins (Ribó et al. 2001; Matteson et al. 2001). In the companion paper, we report the observation that the production of enantiomeric excesses of rotamers of substituted alkanes can be induced by roto-translational motions (vortices), generated by turbomolecular pumping (Lee et al. 2004, 2011a, b). In principle, the direction of rotation of a vortex can act selectively on the direction (and therefore the chirality) of molecular rotation: this affirmation extends the experimental observation that in supersonic beams of gaseous mixtures the component in excess induces directionality and orientation in dragging molecules (Aquilanti et al. 1994), as amply discussed in previous papers (Aquilanti et al. 2011a, and elsewhere).

Control of the orientation of the molecules is a fundamental prerequisite in order that phenomena of chiral selectivity can be demonstrated in processes of photodissociation and molecular dynamics, and that a phenomenology be established of the origin of chirality in chemical reactivity (Aquilanti et al. 2005a). The importance of the molecular orientation was suggested by experiments of diffusion of polarized electrons on thin films of chiral molecules, which are imparted a specific orientation, and by the demonstration of stereodynamical effects in the diffusion of electrons from surfaces of aligned molecules (Ray et al. 1999; Kim et al. 2005; Gerbi et al. 2005); the ionization of chiral molecules by collision with electrons was studied theoretically, showing the dependence from the polarization of the incident electron beam (e.g. Musigmann et al. 2001 and references therein).

Methods to induce alignment and orientation make use of lasers as in single-photon excitation (see for example Weida et al. 1997), high uniform electric fields as in the case of brute force techniques (see for example Bulthuis et al. 1997) or combination of non-uniform and uniform electric fields to align and consequently orient molecules (see for example Hain et al. 1997). This latter technique, which was introduced several decades ago for alignment and rotational state-selection, has been largely used by the Perugia group to investigate the structure and electrical properties of molecules, and by the Osaka group to prepare intense and continuous beams and high duty cycle for crossed beam experiments (see for example Imura et al. 2001a, b, 2003, 2004).

Hexapole fields have been applied mostly on linear and symmetric-top molecules (see an example of applications by the Osaka group: Ohoyama et al. 1995; Hashinokuchi et al. 2003), while in recent years the rising interest for chiral molecules lead us to concentrate our efforts on chiral (and also necessarily asymmetric-top) molecules. In previous work, characterization has been performed of supersonic molecular beams of propylene oxide, C_3H_6O (see Elango et al. 2010, 2011 for the calculation of potential energy surface of the isomerization reactions); for the alignment see Che et al. (2010) and for the orientational distribution, (i.e. the distribution of the angle between the direction of the orienting electric field and component of the permanent dipole moment with respect to one of the three axes of inertia, see Che et al. 2012 and references therein). For the alignment in streams see Aquilanti et al. 1999a, 2011b; Lombardi et al. 2010; Pirani et al. 2001, 2003, 2006, 2007 and Palazzetti et al. (2012).

In this account we focus on the state-of-the-art studies of the manifestations of chirality in photodissociation and molecular collisions. It is well known that photodissociation of enantiomers induced by chiral sources (circularly polarized laser light) leads to the manifestation of chiral effects. Historically, the concept of molecular chirality just originated from observation of the interaction between chiral light and chiral molecules. A significant step forward is the realization of experiments without chiral light, for example by employing unpolarized or simply linearly polarized laser, and to further perform "dark" experiments, inducing the manifestation of chirality in collisions with no use of light sources, but only through molecular collisions: the demonstration would require, for example, an atomic beam and (as a requisite) a beam of oriented chiral molecules.

The paper is structured as follows: in Sect. 2 we discuss the theoretical foundations and present simulation results of the photodissociation of a polyatomic molecule by a linearly polarized laser; the results of trajectory simulations of elastic collision between a structureless atom and an oriented chiral molecule are presented in Sect. 3; conclusions and perspectives about experimental realizations of the model configurations here reported are discussed in Sect. 4. In Appendix, we illustrate the construction and representation of potential energy surfaces of the interactions of rare gasses with prototypical chiral molecules, H_2O_2, and H_2S_2, employed in the molecular dynamics simulations.

2 Photodissociation of aligned molecules

In this section, we discuss the role of molecular orientation in order to obtain chiral effects in photodissociation. This phenomenon, as we mentioned in the introduction, is well known in case of photodissociation with circularly polarized light, i.e. with a chiral source, while it is much less appreciated that similar (chiral) effects can be produced by employing a non-chiral photon source, for example unpolarized or simply linearly polarized laser light.

Interpretation of chiral effects in such processes requires the determination of the vector correlation of photofragments in a molecular (body fixed) reference frame. To this purpose, we adopt a semiclassical vector scheme in the electric dipole approximation and consider a polyatomic molecule with permanent electric dipole **d** in the equilibrium geometry of its electronic ground state (Fig. 1a). We consider a photodissociation process induced by single electronic state excitation of a linearly polarized light, and denote the recoil velocity of the photofragments with **v** and the transition dipole moment with **μ**. The three vectors **v**, **d** and **μ** are defined in the molecular recoil frame *xyz*, where **v** coincides with the *z*-axis. Vectors **v** and **d** define the angle θ ($0 \le \theta \le \pi$), the angle Θ ($0 \le \Theta \le \pi$) is defined by the vectors **v** and **μ**, and ψ is the angle ($0 \le \psi < 2\pi$) defined by the projection of **μ** onto the *xy*-plane and the *x*-axis. For achiral molecules the sign of ψ can indistinctly be either positive or negative, while for chiral molecules, being possible a symmetry breaking, the sign of ψ is characteristic of a specific enantiomer.

A key observation is the sign of ψ can be determined from the photofragment angular distribution of oriented (chiral) molecules via linearly polarized photolysis light. It can be shown that, under sliced imaging condition, θ and ψ can be determined from specific light polarization and orienting field arrangement. Orientation of chiral molecules can be achieved by electric hexapole techniques (see for example Che et al. 2010, 2012). The relation between molecular frame information and experimental observables is described in Rakitzis et al. (2003). Here, we adopt the conventional definition of laboratory coordinates for the sliced imaging detection (Fig. 1b): the time-of-flight axis coincides with the *Z*-axis, the laser propagates along the *Y*-axis and intersects the aligned molecular beam at the center of the ion optics and the events whose velocity lies in the *XY*-plane are those to be detected. The polarization direction of the laser is set at 45° with respect to the *X*-axis in order to obtain information on the θ angle. With the aid of fast high voltage switch, the ion optics for imaging detection can serve also as orienting field providing enough field strength along the time-of-flight axis as demanded for orienting asymmetric-top molecules. In such a way, the photofragment angular distribution of oriented chiral

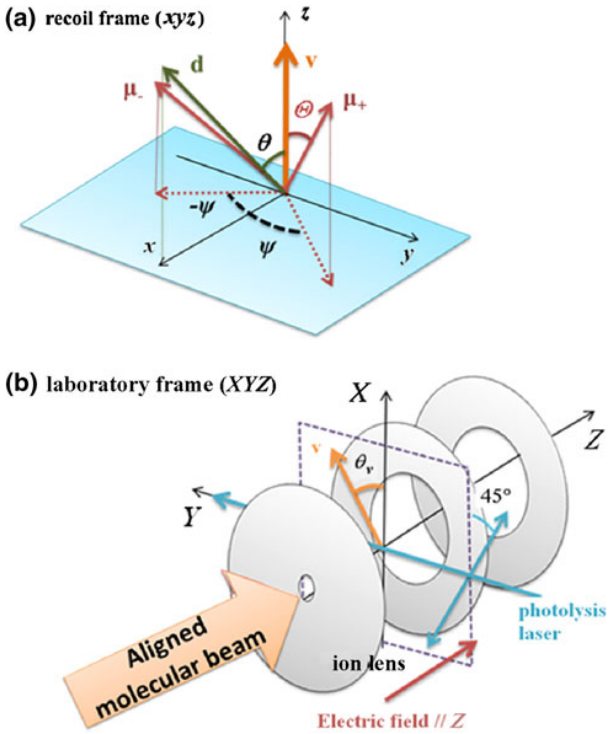

Fig. 1 **a** The vectors and the angular coordinates to describe the angular distribution of the photofragment embedded in the *xyz* Cartesian coordinate frame are illustrated. The origin of the axes is the center-of-mass of the fragment, the *z*-axis is parallel to the direction of the velocity recoil vector **v** and the permanent dipole moment vector **d** is coplanar to the *xz*-plane. The angle between **v** and **d** is indicated by θ ($0 \le \theta \le \pi$), while the angle between **v** and **μ**, the direction of the transition dipole moment vector, is denoted by Θ ($0 \le \Theta \le \pi$). The **μ** vectors are indicated by the subscripts + and − which correspond to the enantiomers. The directions of $\boldsymbol{\mu}_+$ and $\boldsymbol{\mu}_-$, as well as the sign of ψ, the angle between the *x*-axis and the projection of **μ** on the *xy*-plane ($0 \le \psi < 2\pi$), are specific for each enantiomer. **b** The geometry of a photodissociation experiment in the laboratory frame *XYZ* Cartesian coordinate system. The supersonic beam, of molecules which have been previously aligned and state-selected by the hexapole technique, approaches the ion lens through the *Z*-axis, and crosses the photolysis laser whose polarization plane is parallel to the *Y*-axis and tilted by 45° with respect to the *Z*-axis. The deflection angle θ_v denotes the angle formed by the velocity recoil vector **v** and the *X*-axis

molecules acquired via sliced imaging technique can be expressed by the following equation (Rakitzis et al. 2003):

$$
\begin{aligned}
I(\theta_v) = &\left[1 + 2P_2(\cos\Theta)P_2\left(\frac{\cos\theta_v}{\sqrt{2}}\right)\right][1 - c_2P_2(\cos\theta)] \\
&+ 3c_1 \sin\Theta\cos\Theta\sin\theta\cos\theta_v(\cos\psi + \sin\psi\sin\theta_v) \\
&+ \frac{9}{8}c_2\sin^2\Theta\sin^2\theta\left(\frac{1}{2}\cos 2\psi\cos^2\theta_v + \sin 2\psi\sin\theta_v\right)
\end{aligned}
\tag{1}
$$

where θ_v is the angle between the velocity vector **v** and the *X*-axis in the laboratory frame, and c_1 and c_2 are the first

and the second moments of the Legendre expansion in the expression of the orientation distribution (see for example Che et al. 2012 and references therein). In case that the two leading Legendre terms are not sufficient for an accurate description of the orientation distribution, additional expansion coefficients can be included.

As an illustration, we perform a numerical simulation of a model system, demonstrating how one can extract information of molecular chirality from the angular distribution of photofragments. In order to simplify the procedure, we consider a hypothetical chiral molecule with symmetric-top-like orientation distribution behavior (symmetric-top state $|111>$, $c_1 = -0.75$, $c_2 = 0.25$). We assign the following values: $\theta = 45°$, $\Theta = 150°$, and $\psi = \pm 60°$. Figure 2a shows the simulated angular distributions of the two enantiomers and of the racemic mixture of the photodissociated molecule. The two enantiomers present an up-down asymmetric pattern and are seen to shift in opposite directions: such shift corresponds to a tilt of the sliced image data. The shift of angular distribution (and thus the tilt of images) indicates that the value of ψ is different from zero and is a manifestation of the chirality of the molecule. For the racemic mixture (and for achiral molecules) the angular distribution of photofragments is on the contrary symmetric with respect to the *X*-axis (Fig. 2b), since the resultant of **μ** lies on the *xz*-plane (Fig. 2a) and therefore $\psi = 0$

Figure 2a allows us to explain the origin of the tilting of the angular distribution in image results by means of the vector model illustrated in Fig. 1a. We show the situation of a specific molecular orientation corresponding to the maximum excitation probability. In the left panel, the velocity vector **v** (for both achiral and chiral molecules), which is the only one directly detected in imaging experiments, lies in the *XZ*-plane, as well as do both **μ** and **d**. Accordingly, the maximum intensity shows up in the upper side of the sliced image. When **v**, **μ** and **d** are not coplanar (as shown in right panel), the maximum intensity of the image of the chiral molecule is tilted with respect to the *XZ*-plane, either on the right or on the left depending on the handedness of the enantiomer. Note that on the contrary, for achiral molecules or a racemic mixture, even if

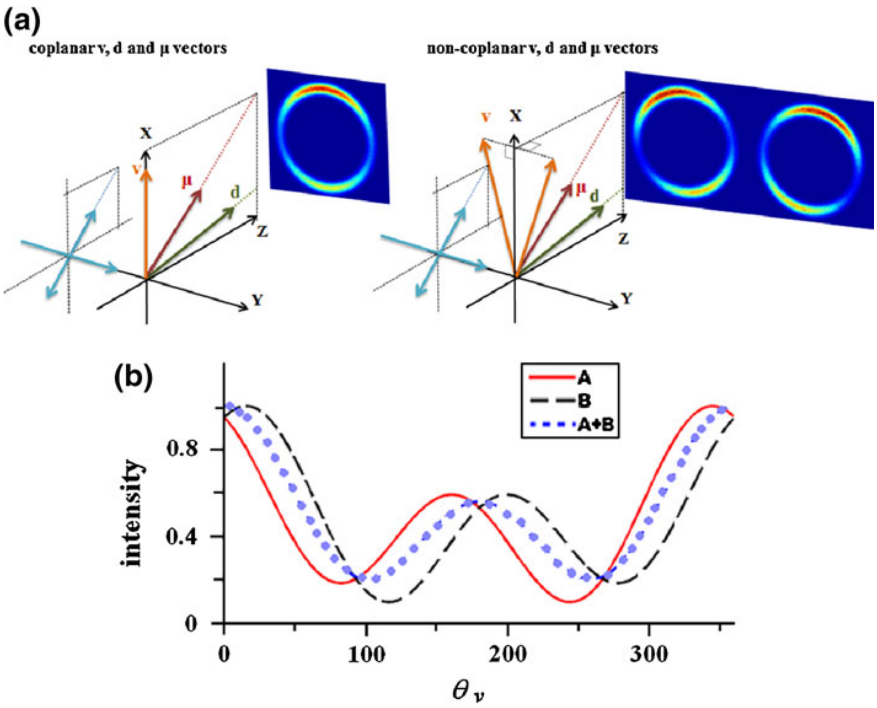

Fig. 2 The figure shows how the correlation of the vectors **v**, **μ** and **d** (for the definition see Fig. 1) leads to different angular distributions for the photofragments from achiral and chiral molecules. In the *left side* of **a**, we report the **v**, **μ** and **d** vectors embedded in the laboratory Cartesian coordinate frame system *XYZ* of a polyatomic achiral molecule, the *blue arrows* representing the polarization plane of the photolysis laser: the corresponding imaging results are seen to show a symmetric distribution of the fragments. In the *right side* of **a**, we illustrate the vector correlation and the corresponding imaging results for each of the two enantiomers of a chiral molecule. In this case the angular distribution of the fragments is non-symmetric. Note that in case of racemic mixtures the angular distribution of the photofragments has the same feature as that described in **a**. In **b**, the corresponding one-dimensional plots of the imaging results shown in **a** are reported. The dependence of the intensity of the signal is illustrated as a function of the deflection angle θ_v. *Continuous* and *dashed curves* are related to the enantiomers (*a* and *b*), while the *dots* describe the racemic mixture ($a + b$) (color figure online)

the vectors are not placed in the same plane, the resulting image possesses the symmetric distribution typical of coplanar vectors (left panel). For references, see for example Rakitzis et al. (2003, 2010) and Krasilnikov et al. (2011) and references therein.

3 Molecular collisions of aligned chiral molecules

Manifestation of chirality in crossed molecular beams, with the use of no light source, can be considered as one of the most fascinating challenges in current research on stereodynamics. The role of the molecular orientation and the presence of three non-coplanar vectors which enforce the chirality of the system has been illustrated in the previous section with reference to Figs. 1 and 2. Here, we present the theoretical background and show the results of the simulation of elastic oriented collisions between a floppy chiral molecule and a rare-gas-atom (specifically, the H_2O_2–Ne system, while in Lombardi et al. 2011 we also report the results for the more rigid H_2S_2 system and details on the trajectory simulations).

An oriented collision is characterized by a molecule (in this case chiral) which is the target of flows of atoms coming from specific directions. The differential cross-section, as a function of the total energy, the angular momentum and initial internal states of the molecule, can be defined and labeled based on the orientation. For a given event i, the directional cross-section is defined as the probability P_i that such event occurs upon an atom-molecule collision at collision energy E, impact parameter b, angles α, β and γ (see the definition of the angles in Appendix; Fig. 3) and internal vibro-rotational states of the semi-rigid molecular rotor v and j:

$$P_i(E,\, b,\, \alpha,\, \beta,\, \gamma,\, v,\, j) = \frac{N_i}{N}, \tag{2}$$

where N_i is the number of times that the event i has been detected in the collision trajectories and N is the total number of trajectories. By integrating over the impact parameters b ($b_{\max}$ is the maximum impact parameter), one obtains the cross-section $\sigma(E,\, \alpha,\, \beta,\, \gamma,\, v,\, j)$:

$$\sigma(E,\, \alpha,\, \beta,\, \gamma,\, v,\, j) = 2\pi \int_{b=0}^{b=b_{\max}} P_i(E,\, b,\, \alpha,\, \beta,\, \gamma,\, v,\, j) b \mathrm{d}b. \tag{3}$$

We also define the function Θ (Φ; E, b, α, β, γ, v, j) which corresponds to the scattering angle, which one would detect in an oriented collision at certain values of E, b, α, β, γ, v, j, and Φ. The variable Φ is an azimuthal angle centered in the center-of-mass of the molecule and spanning the annular ring between b and $b + db$ and

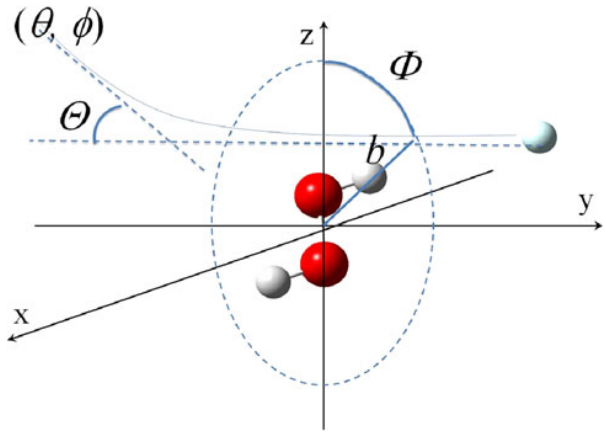

Fig. 3 Geometry of the elastic collision between a rare-gas-atom and the oriented hydrogen peroxide, H_2O_2. The direction of the incoming rare-gas-atom (the projectile) is parallel to the y-axis; the H_2O_2 molecule (the target) is perpendicular to the xy-plane. In the xz-plane a circle is drawn, whose radius is given by the impact parameter b; the intersection point of the trajectory of the incoming atom with the circle defines the Φ angle ($0 \le \Phi < 2\pi$). The initial (incoming) and final (recoil) directions of the rare-gas-atom define the scattering angle Θ ($0 \le \Theta < 2\pi$). The recoil direction is represented by the polar angles θ and ϕ ($0 \le \theta \le \pi$ and $0 \le \phi < 2\pi$) (figure adapted from Lombardi et al. 2011)

perpendicular to the initial velocity of the atom. From Θ (Φ; E, b, α, β, γ, v, j) one can obtain a differential cross-section for oriented collisions, by integrating over b, Φ and γ,

$$I^{v,j}_{\alpha,\beta}(\Theta, E) = 2\pi \int_{b=0}^{b=b_{\max}} \int_{0}^{2\pi} \int_{\gamma_+}^{\gamma_-} \Theta(\Phi; E, b, \alpha, \beta, \gamma, v, j) b \mathrm{d}\gamma \mathrm{d}\Phi \mathrm{d}b, \tag{4}$$

where γ_+ and γ_- are the classical turning points of the internal torsion motion of the molecule (see "Appendix"). Finally, the scattering probability P_Θ at given values of Θ, E, b, α, β, γ, v and j is given by the equation:

$$P_\Theta(E, b, \alpha, \beta, \gamma, v, j) = \int_{0}^{2\pi} \Theta(\Phi; E, b, \alpha, \beta, \gamma, v, j) \mathrm{d}\Phi. \tag{5}$$

The trajectory simulations are carried out by setting as initial conditions a certain impact parameter, the total energy E, the relative orientation of the molecule and the velocity vector of the atom. The initial configuration of the molecule corresponds to that of its minimum energy, while the initial positions and velocities of the atom are varied according to the Φ angle and the orientation of the collision. A sequence of trajectories where the value of Φ varies for a small range from 0 to 2π has been calculated in order to reproduce the effects of a rotating flow of

incoming atoms at the fixed initial conditions. Figure 4 shows results of the trajectory simulations performed for the H_2O_2–Ne system (for the H_2S_2–Ne system see Lombardi et al. 2011). In Fig. 4a, we report the variation of the scattering angle Θ as a function of Φ for the two enantiomers of the hydrogen peroxide. The initial conditions are a collision energy of 20 kcal/mol, impact parameter of 1.0 Å and $\beta = 0$. In Fig. 4b, we show the variation of the recoil angle ϕ as function of the other recoil angle Θ and of the Φ angle, at a collision energy of 120 kcal/mol, while the impact parameter and β have the same value as previously. Both figures show the effect of the different enantiomers (+) and (−) on the scattering angle. In particular, Fig. 4b shows how the change of the chirality sign of the target molecule can be seen as a change in the handedness of the Cartesian reference system.

In Fig. 5, we show the relationship between the angular coordinates introduced in this section and the coordinates used to describe the photodissociation process (see Sect. 2). This case is verified if **ε**, the light polarization vector, and **μ** have the same direction and happens in case of maximum excitation probability. Both the angles Φ and ψ carry information on molecular chirality, but with a slight

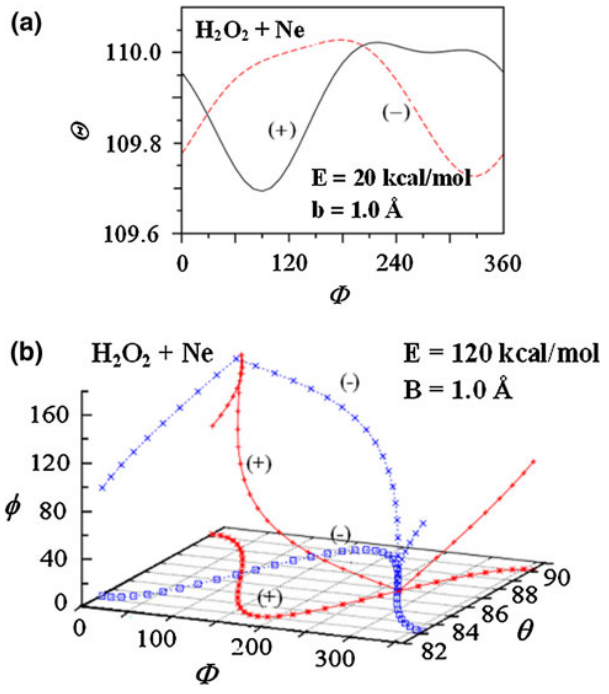

Fig. 4 **a** The scattering angle Θ as a function of Φ angle for the H_2O_2–Ne system, for elastic collisions carried out at 20 kcal/mol and impact parameter $b = 1.0$ Å. The signs (+) and (−) are referred to the two enantiomers. **b** The recoil angles θ and ϕ as function of the angle Θ for the elastic collision H_2O_2–Ne with energy 120 kcal/mol and impact parameter $b = 1.0$ Å (figure adapted from Lombardi et al. 2011)

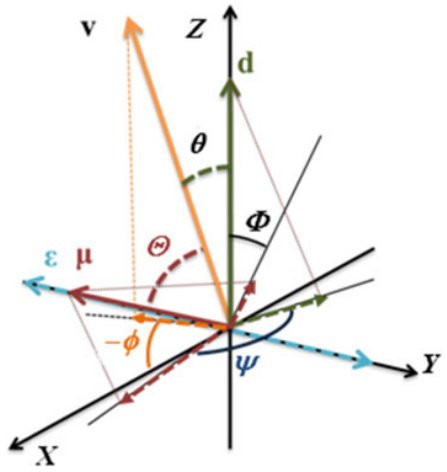

Fig. 5 Standardization of the angular coordinates defined in Sect. 2 for the angular distribution of the photofragment and the angular coordinates defined in Sect. 3 to describe an elastic collision between the Ne atom and the H_2O_2 molecule. The *figure* shows the correspondence of the two systems under conditions of maximum excitation probability, i.e. when **ε**, the polarization vector of light, and **μ** have the same direction

difference on their own definition: the normal of the plane which defined Φ or ψ is either the incoming vector in full collision (molecular collision) or the outgoing vector (**v**) in the half collision (photodissociation).

4 Conclusions

In this paper and the previous one in this series, we have provided a collection of reports about the state-of-art of the manifestation of chirality in processes involving aligned molecules in the gas phase.

The investigation of the issue of chiral effects in collisions is demonstrated important and needs to be tackled. Although theory allows us to make predictions, experimental investigation is at an early stage of realization (see however Su et al. 2013). The manifestation of enantioselective processes requires that the molecules are oriented and that the experimental arrangement consists of three non-coplanar vectors which endorse a chiral frame to the system. We have seen that an ample experimental know-how has been accumulated regarding the use of hexapole fields for the alignment and orientation of molecules. In more recent years, efforts have been devoted to the characterization of supersonic beams of oriented chiral, and thus asymmetric-top molecules. The choice of working with supersonic molecular beams and hexapoles relies on the opportunity of producing intense beams with a high duty cycle, suitable for photodissociation and collision experiments (see for example Aquilanti et al. 1995, 1997, 1998, 1999b, c; Cappelletti et al. 2002, 2006a, b).

The importance of molecular orientation in the stereodynamics of chiral molecules has been described in Sect. 2, where we have shown the angular distribution in the simulation of a photodissociation process of a chiral molecule, and in Sect. 3 where we have reported the scattering angle and the recoil angles as a function of the Azimuthal angle Φ. The connection between the two configurations is an interesting result of this paper. Sections 2 and 3 show through the analysis of vector correlation and establishing the correspondence of the angular variables in the case of the photodissociation to those defined for the molecular collisions, common nature of the manifestation of chiral effects in both cases, evidenced by the simulations. The ψ angle, defined in Sect. 2 as the angle formed by the projection of the dipole moment vector $\boldsymbol{\mu}$ onto the xy-plane and the x-axis, denotes the chirality of the molecule, its sign is in fact characteristic of each enantiomer, because of the presence of an improper rotation axis. The same role is played, in case of elastic collisions, by the Φ angle.

Acknowledgments A. L. and F. P. acknowledge financial support from MIUR PRIN 2010–2011 (contract 2010ERFKXL_002) and from Phys4entry FP7 2007-2013 (contract 242311) respectively. V. A. and F. P. wish to thank the friendly hospitality and the warm scientific atmosphere provided by Professor King-Chuen Lin, his group and visiting Professor Toshio Kasai at the Department of Chemistry of the National Taiwan University.

Appendix: interaction of rare gasses with the chiral molecules H_2O_2 and H_2S_2

Interactions of simple chiral molecules are of general interest, and of particular use in simulations such as those described in Sect. 3. Experimental studies by crossed molecular beams on the interactions (providing essentially the component of the isotropic forces) between H_2O (Aquilanti et al. 2005b) and H_2S (Cappelletti et al. 2006c) with rare gas atoms provided the ground for theoretical investigations on complementary information on the related anisotropies (Aquilanti et al. 2002a, b, 2003, 2005b). Similar studies on H_2O_2 and H_2S_2 (among the simplest chiral molecules) are of interest, in view of rising attention on chirality in molecular dynamics, although experiments are still lacking. Future implementation of such experiments, motivated the study of potential energy surfaces of the interaction between the floppy (chiral) molecules H_2O_2 and H_2S_2 with rare gas atoms, generated by quantum chemical calculations (Maciel et al. 2006, 2007a, b; Ragni et al. 2007; Bitencourt et al. 2008; Aquilanti et al. 2009), and hyperspherical harmonics representations which enforce compactness and full account of the symmetry of the systems (Aquilanti et al. 2000, 2001; Lombardi et al. 2007, see also Barreto et al. 2009, 2012a, b). These results permitted the simulations of elastic collisions with chirality change, reported in Sect. 3.

Floppy molecules have a rigid structure and the only active vibrational mode is the torsional one. A proper choice of coordinates is desirable for a faithful representation of geometrical and symmetry properties of the systems. As shown in Fig. 6, the system is described by four coordinates: the distance between the rare gas atom and the center-of-mass of the molecule r, the spherical angles α and β, which are the azimuth and the elevation respectively and vary between 0 and 2π and between 0 and π. The dihedral angle of the molecule is denoted by γ and its value is included between 0 and 2π. The range of the angular variables spans a three-dimensional manifold isomorphic to S^3, thus the proper orthonormal expansion basis set is that of hyperspherical harmonics.

Quantum chemical calculations have been employed to optimize the molecular geometries at three values of γ: 0, corresponding to the *cis* geometry; π, *trans* geometry and finally the equilibrium geometry corresponding to $\gamma = 112.54°$ for H_2O_2 and $\gamma = 91.05°$ for H_2S_2. A certain number of points of the potential energy surfaces of various distances r, for some different sets of the angular coordinates, have been determined by ab initio calculations (for details on ab initio calculations see Barreto et al. 2007; Maciel et al. 2008).

The interaction potential $V(r; \alpha, \beta, \gamma)$ is thus expressed by the following expansion:

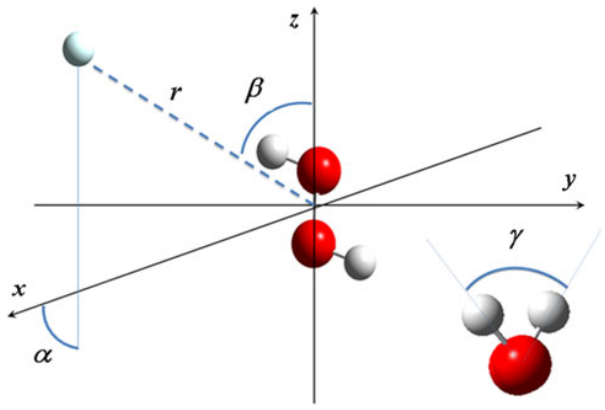

Fig. 6 The coordinates of the H_2O_2, rare-gas-atom system embedded in the xyz Cartesian coordinate frame. The z-axis is parallel to the Jacobi vector of the molecule and its center-of-mass coincides with the origin of the frame. The system is described by a radial coordinate r which represents the distance between the center-of-mass of the molecule and the rare-gas-atom and by three angular coordinates: the spherical angles α, the azimuth ($0 \leq \alpha \leq 2\pi$), and β, the elevation ($0 \leq \beta \leq \pi$), which denote the orientation of the rare-gas-atom with respect to the center-of-mass of the molecule. The third angular coordinate, γ ($0 \leq \gamma \leq 2\pi$), is reported in the *lower right corner*, where we show a view (from the z-axis), and describe the torsion angle of the molecule (figure adapted from Barreto et al. 2007)

$$V(r;\,\alpha,\,\beta,\,\gamma) = \sum_{\mu} v^{\mu}_{\mathrm{MM}\prime}(r) R^{\mu}_{\mathrm{MM}\prime}(\alpha,\,\beta,\,\gamma) \qquad (6)$$

where μ, M and M' are indexes of the expansion whose value is an integer positive number (including 0), $v(r)$ are the expansion moments and $R(\alpha,\,\beta,\,\gamma)$ are real hyperspherical harmonics, which are obtained as a linear combination of the Wigner D-functions. Details on the determination of the expansion moments, on the real hyperspherical harmonics and on the construction of the potential energy surfaces are reported in Barreto et al. 2007, 2011; Maciel et al. 2008; Palazzetti et al. 2011).

References

Aquilanti V, Maciel GS (2006) Observed molecular alignment in gaseous streams and possible chiral effects in vortices and surface scattering. Orig Life Evol Biosph 36:435–441

Aquilanti V, Ascenzi D, Cappelletti D, Pirani F (1994) Velocity dependence of collisional alignment of oxygen molecules in gaseous expansions. Nature 371:399–402

Aquilanti V, Ascenzi D, Cappelletti D, Franceschini S, Pirani F (1995) Scattering of rotationally aligned oxygen molecules and the measurement of anisotropies of van der Waals forces. Phys Rev Lett 74:2929–2932

Aquilanti V, Ascenzi D, Cappelletti D, Fedeli R, Pirani F (1997) Molecular beam scattering of nitrogen molecules in supersonic seeded beams: a probe of rotational alignment. J Phys Chem A 101:7648–7656

Aquilanti V, Ascenzi D, Cappelletti D, De Castro M, Pirani F (1998) Scattering of aligned molecules. The potential energy surfaces for the Kr–O_2 and the Xe–O_2 systems. J Chem Phys 109:3898–3910

Aquilanti V, Ascenzi D, de Castro Vitores M, Pirani F, Cappelletti D (1999a) A quantum mechanical view of molecular alignment and cooling in seeded supersonic expansion. J Chem Phys 111:2620–2632

Aquilanti V, Ascenzi D, Bartolomei M, Cappelletti D, Cavalli S, de Castro Vitores M, Pirani F (1999b) Quantum interference scattering of aligned molecules: bonding in O_4 and role of spin coupling. Phys Rev Lett 82:69–72

Aquilanti V, Ascenzi D, Bartolomei M, Cappelletti D, Cavalli S, de Castro Vitores M, Pirani F (1999c) Molecular beam scattering of aligned oxygen molecules. The nature of the bond in the O_2–O_2 Dimer. J Am Chem Soc 121:10794–10802

Aquilanti V, Beddoni A, Cavalli S, Lombardi A, Littlejohn R (2000) Collective hyperspherical coordinates for polyatomic molecules and clusters. Mol Phys 98:1763–1770

Aquilanti V, Bartolomei M, Cappelletti D, Carmona-Novillo E, Pirani F (2001) Dimers of the major components of the atmosphere: realistic potential energy surfaces and quantum mechanical prediction of spectral features. Phys Chem Chem Phys 3:3891–3894

Aquilanti V, Bartolomei M, Cappelletti D, Carmona-Novillo E, Pirani F (2002a) The N_2–N_2 system: an experimental potential energy surface and calculated rotovibrational levels of the molecular nitrogen dimer. J Chem Phys 117:615–627

Aquilanti V, Carmona-Novillo E, Pirani F (2002b) Quantum mechanics of molecular oxygen clusters: rotovibrational dimer dynamics from realistic potential energy surfaces. Phys Chem Chem Phys 4:4970–4978

Aquilanti V, Bartolomei M, Carmona Novillo E, Pirani F (2003) The asymmetric dimer N2–O2: characterization of the potential energy surface and quantum mechanical calculation of rotovibrational levels. J Chem Phys 118:2214–2222

Aquilanti V, Bartolomei M, Pirani F, Cappelletti D, Vecchiocattivi F, Shimizu Y, Kasai T (2005a) Orienting and aligning molecules for stereochemistry and photodynamics. Phys Chem Chem Phys 7:291–300

Aquilanti V, Cornicchi E, Teixidor MM, Saendig N, Pirani F, Cappelletti D (2005b) Glory scattering measurement of water–noble-gas interactions: the birth of the hydrogen bond. Angew Chem Int Ed 44:2356–2359; Angew Chem 117:2408–2412

Aquilanti V, Grossi G, Lombardi A, Maciel GS, Palazzetti F (2008) The origin of chiral discrimination: supersonic molecular beam experiments and molecular dynamics simulations of collisional mechanisms. Phys Scr 78:058119–058125

Aquilanti V, Ragni M, Bitencourt ACP, Maciel GS, Prudente F (2009) Intramolecular dynamics of RS–SR0 Systems (R, R0 = H, F, Cl, CH3, C2H5): torsional potentials, energy levels, partition functions. J Phys Chem A 113:3804–3813

Aquilanti V, Grossi G, Lombardi A, Maciel GS, Palazzetti F (2011a) Aligned molecular collisions and a stereodynamical mechanism for selective chirality. Rend Fis Acc Lincei 22:125–135

Aquilanti V, Schettino V, Zerbi G (2011b) Introduction: astrochemistry—molecules in space and in time. Rend Fis Acc Lincei 22:67–68

Avalos A, Babiano R, Cintas P, Jiménez JL, Palacios JC (1998) Absolute asymmetric synthesis under physical fields: facts and fictions. Chem Rev 98:2391–2404

Bacchus-Montabonel MC (2011) Radiative and collisional processes in space chemistry. Rend Fis Acc Lincei 22:95–103

Barreto PRP, Vilela AFA, Lombardi A, Maciel GS, Palazzetti F, Aquilanti V (2007) The hydrogen-peroxide-rare-gas systems: quantum chemical calculations and hyperspherical harmonic representation of the potential energy surface for atom–floppy-molecule interactions. J Phys Chem A 111:12754–12762

Barreto PRP, Ribas VW, Palazzetti F (2009) Potential energy surface for the H_2O–H_2 system. J Phys Chem A 113:15047–15054

Barreto PRP, Albernaz AF, Palazzetti F, Lombardi A, Grossi G, Aquilanti V (2011) Hyperspherical representation of potential energy surfaces: intermolecular interactions in tetra-atomic and penta-atomic systems. Phys Scr 84:028111

Barreto PRP, Albernaz AF, Palazzetti F (2012a) Potential energy surfaces for van der Waals complexes of rare gases with H_2S and H_2S_2: extension to xenon interactions and hyperspherical harmonics representation. Int J Quant Chem 112:834–847

Barreto PRP, Albernaz AF, Capobianco A, Palazzetti F, Lombardi A, Grossi G, Aquilanti V (2012b) Potential energy surfaces for interactions of H_2O with H_2, N_2 and O_2: a hyperspherical harmonics representation, and a minimal model for the H_2O–rare-gas-atom systems. Comp Theor Chem 990:53–61

Barron LD (1986) True and false chirality and absolute asymmetric synthesis. J Am Chem Soc 108:5539–5542

Barron LD (2013) True and false chirality and absolute enantioselection. Rend Fis Acc Lincei. doi:10.1007/s12210-013-0224-6

Bitencourt ACP, Ragni M, Maciel GS, Aquilanti V, Prudente F (2008) Level distributions, partition functions and rates of chirality changing processes for the torsional mode around O–O bonds. J Chem Phys 129:154316–154324

Bulthuis J, Möller J, Loesch HJ (1997) Brute force orientation of asymmetric top molecules. J Phys Chem A 101:7684–7690

Cappelletti D, Bartolomei M, Pirani F, Aquilanti V (2002) Molecular beam scattering on benzene-rare gas systems: probing the potential energy surfaces for the C_6H_6–He, –Ne and –Ar dimers. J Phys Chem A 106:10764–10772

Cappelletti D, Bartolomei M, Aquilanti V, Pirani F, Demarchi G, Bassi D, Iannotta S, Scotoni M (2006a) Alignment of ethylene molecules in supersonic seeded expansions probed by infrared polarized laser absorption and by molecular beam scattering. Chem Phys Lett 420:47–53

Cappelletti D, Bartolomei M, Aquilanti V, Pirani F (2006b) A molecular beam scattering study of weakly bound complexes: the potential energy surfaces for the C_2H_4–Ar and –Kr systems. Chem Phys Lett 420:100–105

Cappelletti D, Vilela AFA, Barreto PRP, Gargano R, Pirani F, Aquilanti V (2006c) Intermolecular interactions of H2S with rare gases from molecular beam scattering in the glory regime and from ab initio calculation. J Chem Phys 125:133111–133118

Che DC, Palazzetti F, Okuno Y, Aquilanti V, Kasai T (2010) Electrostatic hexapole state-selection of the asymmetric—top molecule propylene oxide. J Phys Chem A 114:3280–3286

Che DC, Kanda K, Palazzetti F, Aquilanti V, Kasai T (2012) Electrostatic hexapole state-selection of the asymmetric-top molecule propylene oxide: rotational and orientational distributions. Chem Phys 399:180–192

Elango M, Maciel GS, Palazzetti F, Lombardi A, Aquilanti V (2010) Quantum chemistry of C_3H_6O molecules: structure and stability, isomerization pathways, and chirality changing mechanisms. J Phys Chem A 114:9864–9874

Elango M, Maciel GS, Lombardi A, Cavalli S, Aquilanti V (2011) Quantum chemical and dynamical approaches to intra and intermolecular kinetics: the $CnH_2nO(n = 1, 2, 3)$ molecules. Int J Quant Chem 111:1784–1791

Gallori E (2011) Astrochemistry and the origin of genetic material. Rend Fis Acc Lincei 22:113–118

Gerbi A, Vattuone L, Rocca M, Valbusa U, Pirani F, Cappelletti D, Vecchiocattivi F (2005) Stereodynamic effects int he adsorption of propylene molecules on Ag(001). J Phys Chem B 109:22884–22889

Hain TD, Weibel MA, Backstrand KM, Curtiss TJ (1997) Rotational state selection and orientation of OH and OD radicals by electric hexapole beam-focusing. J Phys Chem A 101:7674–7683

Hashinokuchi M, Che DC, Watanabe D, Fukuyama T, Koyano I, Shimizu I, Woelke A, Kasai T (2003) Single $|J\Omega M_J\rangle$state-selection of OH radicals using an electrostatic hexapole field. Phys Chem Chem Phys 5:3911–3915

Imura K, Kawashima T, Ohoyama H, Kasai T, Nakajima A, Kaya K (2001a) Non-destructive selection of geometrical isomers of the $Al(C_6H_6)$ cluster by a 2 m electrostatic hexapole field. Phys Chem Chem Phys 3:3593–3597

Imura K, Kawashima T, Ohoyama H, Kasai T (2001b) Direct determination of the permanent dipole moments and structures of AI–CH_3CN and AI–NH_3 by using 2-m electrostatic hexapole field. J Am Chem Soc 123:6367–6371

Imura K, Ohoyama H, Kasai T (2003) Metal-ligand interaction of Ti–C_6H_6 complex size-selected by a 2-m long electrostatic hexapole field. Chem Phys Lett 369:55–59

Imura K, Ohoyama H, Kasai T (2004) Structures and its dipole moments of half-sandwich type metal–benzene (1:1) complexes determined by 2-m long electrostatic hexapole. Chem Phys 301:183–187

Kim JW, Carbone M, Dil JH, Tallarida M, Flammini R, Casaletto MP, Horn K, Piancastelli MN (2005) Atom-specific identification of adsorbed chiral molecules by photoemission. Phys Rev Lett 95:107601–107604

Krasilnikov MB, Kuznetsov VV, Suits AG, Vasyutinskii OS (2011) Vector correlations in photodissociation of polarized polyatomic molecules beyond the axial recoil limit. Phys Chem Chem Phys 13:8163–8174

Lee HN, Su TM, Chao I (2004) Rotamer dynamics of substituted simple alkanes. 1. A classical trajectory study of collisional orientation and alignment of 1-bromo-2-chloroethane with argon. J Phys Chem A 108:2567–2575

Lee HN, Chang LC, Su TM (2011a) Optical rotamers of substituted simple alkanes induced by macroscopic translation-rotational motions. Chem Phys Lett 507:63–68

Lee HN, Chao I, Su TM (2011b) Asymmetry in the internal energies of the optical rotamers of 1-bromo-2-chloroethane in oriented-molecule/surface scattering: a classical molecular dynamics study. Chem Phys Lett 517:132–138

Lombardi A, Palazzetti F, Peroncelli L, Grossi G, Aquilanti V, Sevryuk MB (2007) Few-body quantum and many-body classical hyperspherical approaches to reactions and to cluster dynamics. Theor Chem Acc 117:709–721

Lombardi A, Maciel GS, Palazzetti F, Grossi G, Aquilanti V (2010) Alignment and chirality in gaseous flows. J Vacuum Soc Jpn 53:645–653

Lombardi A, Palazzetti F, Maciel GS, Aquilanti V, Sevryuk MB (2011) Simulation of oriented collision dynamics of simple chiral molecules. Int J Quant Chem 111:1651–1658

Longo S, Coppola CM (2013) Stochastic models of chiral symmetry breaking in autocatalytic networks with anomalous fluctuations. Rend Fis Acc Lincei. doi:10.1007/s12210-013-0234-4

Maciel GS, Bitencourt ACP, Ragni M, Aquilanti V (2006) Studies of the dynamics around the O–O bond: orthogonal local modes of hydrogen peroxide. Chem Phys Lett 432:383–390

Maciel GS, Bitencourt ACP, Ragni M, Aquilanti V (2007a) Alkyl peroxides: effect of substituent groups on the torsional mode around the O–O bond. Int J Quant Chem 107:2697–2707

Maciel GS, Bitencourt ACP, Ragni M, Aquilanti V (2007b) Quantum study of peroxidic bonds and torsional levels for ROOR' molecules (R, R' = H, F, Cl. NO, CN). J Phys Chem A 111:12604–12610

Maciel GS, Barreto PRP, Palazzetti F, Lombardi A, Aquilanti V (2008) A quantum chemical study of H_2S_2: intramolecular torsional mode and intermolecular interactions with rare gases. J Chem Phys 129:164302–164311

Matteson DS, Ribó JM, Crusats J, Sagués F, Claret J, Rubires R (2001) Chiral selection when stirred, not shaken. Science 293:1435

Musigmann M, Busalla A, Blum K, Thompson DG (2001) Enantio-selective collisions between unpolarized electrons and chiral molecules. J Phys B 34:L79–L85

Ohoyama H, Ogawa T, Kasai T (1995) A single rotational state analysis of the state-selected CH_3I beam: a new Monte Carlo simulation including the second-order Stark effect. J Phys Chem A 99:13606–13610

Palazzetti F, Elango M, Lombardi A, Grossi G, Aquilanti V (2011) Spherical and hyperspherical representation of potential energy surfaces for intermolecular interactions. Int J Quant Chem 111:318–332

Palazzetti F, Maciel GS, Lombardi A, Grossi G, Aquilanti V (2012) The astrochemical observatory: molecules in the laboratory and in the cosmos. J Chin Chem Soc 59:1045–1052

Pirani F, Cappelletti D, Bartolomei M, Aquilanti V, Scotoni M, Vescovi M, Ascenzi D, Bassi D (2001) Orientation of benzene in supersonic expansions, probed by IR-laser absorption and by molecular beam scattering. Phys Rev Lett 86:5035–5038

Pirani F, Bartolomei M, Aquilanti V, Scotoni M, Vescovi M, Ascenzi D, Bassi D, Cappelletti D (2003) Collisional orientation of the benzene molecular plane in supersonic seeded expansions, probed by infrared polarized laser absorption spectroscopy and by molecular beam scattering. J Chem Phys 119:265–276

Pirani F, Maciel GS, Cappelletti D, Aquilanti V (2006) Experimental benchmarks and phenomenology of interatomic forces: open shell and electronic anisotropy effect. Int Rev Phys Chem 25:165–199

Pirani F, Cappelletti D, Bartolomei M, Aquilanti V, Demarchi G, Tosi P, Scotoni M (2007) The collisional alignment of acetylene molecules in supersonic seeded expansions probed by infrared absorption and molecular beam scattering. Chem Phys Lett 437:176–182

Quack M (2002) How important is parity violation for molecular and biomolecular chirality? Angew Chem Int Ed 41:4618–4630

Ragni M, Bitencourt ACP, Aquilanti V (2007) Orthogonal coordinates for the dynamics of four bodies and for the representation of potentials of tetra-atomic molecules. Int J Quant Chem 107:2870–2888

Rakitzis TP, Janssen MHM (2010) Photofragment angular momentum distributions from oriented and aligned polyatomic molecules: beyond the axial recoil limit. Mol Phys 108:937–944

Rakitzis TP, Van den Brom AJ, Janssen MHM (2003) Molecular and laboratory frame photofragment angular distribution from oriented and aligned molecules. Chem Phys Lett 372:187–194

Ray K, Ananthavel SP, Waldeck DH, Naaman R (1999) Asymmetric scattering of polarized electrons by organized organic films of chiral molecules. Science 283:814–816

Ribó JM, Crusats J, Sagués F, Claret J, Rubires R (2001) Chiral sign induction by vortices during the formation of mesophases in stirred solutions. Science 292:2063–2066

Ribó JM, El-Hachemi Z, Crusats J (2013) Effect of flows in auto-organization, self-assembly, and emergence of chirality. Rend Fis Acc Lincei. doi:10.1007/s12210-013-0233-5

Rikken GLJA, Raupach E (2000) Enantioselective magnetochiral photochemistry. Nature 405:932–935

Su TM, Palazzetti F, Lombardi A, Grossi G, Aquilanti V (2013) Molecular alignment and chirality in gaseous streams and vortices. doi:10.1007/s12210-013-0249-x

Weida MJ, Parmenter CS (1997) Aligning symmetric and asymmetric top molecules via single photon excitation. J Chem Phys 107(7138):7147